Aquatic Sciences (2018) 80:29
https://doi.org/10.1007/s00027-018-0580-5

Aquatic Sciences

RESEARCH ARTICLE

Spatio-temporal variability and controls on methane and nitrous oxide in the Guadalquivir Estuary, Southwestern Europe

I. Emma Huertas[1] · Susana Flecha[1] · Gabriel Navarro[1] · Fiz F. Perez[2] · Mercedes de la Paz[3]

Received: 9 October 2017 / Accepted: 21 April 2018 / Published online: 28 April 2018

Abstract

Estuaries are significant methane (CH_4) and nitrous oxide (N_2O) emitters, although dynamics of both greenhouse gases in these ecosystems are regulated by complex processes. In this work, we aimed at characterizing the spatio-temporal distribution of CH_4 and N_2O in the Guadalquivir river estuary (SW Spain), the southernmost European estuary. During eight sampling cruises conducted between 2016 and 2017, surface water CH_4 and N_2O concentrations were measured along the salinity gradient of the estuary by using static-head space equilibration gas chromatography. The CH_4 and N_2O saturation ranges over the estuarine transect were 520–30,800% (average 2285%) and 40–390% (average 183%), respectively and air–water fluxes ranged from 13 to 1000 µmol m^{-2} day^{-1}(average 66.2 µmol m^{-2} day^{-1}) for CH_4 and from −7 to 35 µmol m^{-2} day^{-1} (average 8.5 µmol m^{-2} day^{-1}) for N_2O. A slight increase in the emissions was detected upstream and no seasonal trends were observed. Mixing between freshwater and oceanic waters influenced biogeochemistry of estuarine waters, affecting CH_4 and N_2O fluxes. In order to identify potential sources of CH_4 and N_2O, biogeochemical parameters involved in the formation pathways of both gases, such as salinity, dissolved oxygen, nutrients and organic matter were analyzed. Results suggested that sulfate inhibition and microbial oxidation played a relevant role in dissolved CH_4 accumulation in the water column whereas associations found between N_2O, nitrate and oxygen indicated that nitrification was a major source of this gas. Therefore, the influence of the tidal-fluvial interaction on ecosystem metabolism regulates trace gas dynamics in the Guadalquivir estuary.

Keywords Estuary · Guadalquivir · Methane · Nitrification · Nitrous oxide

Introduction

Methane (CH_4) and nitrous oxide (N_2O) are important atmospheric greenhouse gases, as they absorb infrared radiation at higher efficiencies per molecule than carbon dioxide (CO_2) and participate in atmospheric chemical reactions that lead to changes in stratospheric ozone (Myhre et al. 2013; Ravishankara et al. 2009). According to the last Intergovernmental Panel for Climate Change (IPPC) report, in 2011 the global average atmospheric dry mole fractions of CH_4 and N_2O were ~1803 and ~324 ppb, which exceeded the pre-industrial levels by about 150%, and 20%, respectively (Ciais et al. 2013). Even though the atmospheric growth rate of both gases shows a marked interannual variability (Nisbet et al. 2016; Thompson et al. 2017), evidence indicates that they will continue rising due to numerous sources.

Major anthropogenic CH_4 sources are agricultural practices, emissions from fossil fuel extraction, landfills and waste and the large increase in ruminants. Natural sources include anaerobic aquatic environments where biogenic methane is formed, such as wetlands, freshwater lakes, streams and rivers, estuarine and coastal regions, but also areas of thermogenic methane release, geothermal vents, and natural biomass combustion (Hamdan and Wickland 2016). Recent studies have concluded that the rapid atmospheric methane rise detected over the last decade is a result of increased emissions from biogenic sources (Nisbet et al. 2016; Schaefer et al. 2016), particularly in the tropics, which can be linked to expanding tropical wetlands in response to positive rainfall anomalies (Nisbet et al. 2016). Comparison

✉ I. Emma Huertas
emma.huertas@icman.csic.es

[1] Instituto de Ciencias Marinas de Andalucía, (CSIC), Polígono Río San Pedro s/n, Puerto Real, 11519 Cádiz, Spain

[2] Instituto de Investigaciones Marinas (CSIC), Rúa de Eduardo Cabello 6, 36208 Vigo, Spain

[3] Centro Oceanográfico de A Coruña (IEO), Paseo Marítimo Alcalde Francisco Vázquez 10, 15001 A Coruña, Spain

with historic methane formation suggests that if the methane growth driven by this type of biogenic emissions continues rising, the present increase will be beyond the largest events in the last millennium (Nisbet et al. 2016).Therefore, the assessment of CH_4 release from wetlands and other inland waters is particularly relevant to gain insights on production and emission pathways and reduce uncertainty in the global methane budget (Kirschke et al. 2013). Current uncertainties are attributable to the choice of methodology, as top–down and bottom–up methods result in marked differences in the inventories (Saunois et al. 2016), the approach selected to compute the emissions, discrepancies in surface areas and bias in the geographic distribution of the aquatic systems studied so far. Measurements of methane emissions from aquatic environments have been concentrated in wetlands, freshwater lakes, reservoirs, and fluvial systems whereas reports on methane emissions from estuaries are still relatively sparse (Hamdan and Wickland 2016). Several works have proven that estuaries make a significant contribution to CH_4 emissions (Borges and Abril 2011; Cotovicz et al. 2016; Gelesh et al. 2016), globally releasing between 1 and 7 Tg CH_4 $year^{-1}$(Borges et al. 2016), which is comparable, for instance, to methane fluxes arising from the open ocean domain (< 2 Tg CH_4 $year^{-1}$, Borges et al. 2016). In fact, methane supersaturation higher than 20,000% is a frequent phenomenon in estuarine waters (Abril and Iversen 2002; Ferrón et al. 2007; Middelburg et al. 2002; Upstill-Goddard et al. 2000), where the gas mostly originates from freshwater inputs and in situ sediment methanogenesis (Borges et al. 2015b). Local CH_4 production related to high turbidity in the water column has been also suggested in two British estuaries (Upstill-Goddard et al. 2000). On the other hand, a decrease in dissolved CH_4 in turbid waters has been reported in some European estuaries, which has been attributed to accelerated CH_4 outgassing due to high turbulence or to increased CH_4 oxidation by suspended mater particles-attached bacteria (Middleburg et al. 2002, Abril et al. 2007). Currently, there is significant evidence indicating that estuarine CH_4 production comes from sediments (inter-tidal or sub-tidal) from where it diffuses to the water column (Borges and Abril 2011 and references therein). Regardless of the methane source, there is a strong need for more methane emission data in estuarine systems to further constrain global methane budget (Saunois et al. 2016).

Estuaries have been also recognized as a significant source of N_2O to the atmosphere (Bange 2006; Barnes and Upstill-Goddard 2011; Murray et al. 2015), emitting about 0.25 Tg N $year^{-1}$(Bakker et al. 2014). N_2O is produced by microbial processes, such as nitrification (oxidation of ammonium to nitrate) and denitrification (reduction of nitrate to N_2), with the yield of N_2O formation during both mechanisms being strongly dependent upon dissolved oxygen (DO) concentration. These coastal systems receive high loads of nitrogen (N) that fuel both formation pathways and promote eutrophication, which leads to hypoxia or anoxia (Howarth et al. 2011), conditions that ultimately regulate N_2O release (Bakker et al. 2014; Naqvi et al. 2010). Eutrophic European estuaries are considered net N_2O emitters (Stocker et al. 2013) although additional investigations are needed to allow for more accurate continental and global budgeting of the emissions.

Here, we present the results of the first measurements of dissolved N_2O and CH_4 along the Guadalquivir river estuary (SW Spain) during 2016 and 2017. The estuary (Fig. 1) has undergone an intense anthropogenic pressure since the second half of the twentieth century that has led to profound alterations in its original morphology and ecological conditions (Ruiz et al. 2015). Agriculture and surrounding large population settlements introduce considerable inputs of nutrients, organic matter and inorganic compounds, which result in a strong limitation in light availability for primary production (Ruiz et al. 2015, 2017). The composition of the drainage basin of a siliceous origin in the north and a carbonate part in the south also contributes to the high concentration of suspended solids and dissolved carbonates characteristic of these estuarine waters (de la Paz et al. 2007). High turbidity promotes net heterotrophy, leading to a strong CO_2 supersaturation and the ecosystem behaves as a massive CO_2 emitter (Flecha et al. 2015). Accordingly, events of hypoxia are common in the estuary, especially in its inner part, where DO levels as low as 34 µmol kg^{-1} have been measured (Flecha et al. 2015).

Our study was aimed at (1) characterizing N_2O and CH_4 distribution and their saturations along the Guadalquivir estuary, (2) providing the first estimates of air–water exchange of both gases and (3) identifying potential production pathways. Moreover, our data can be used to complement the overall diagnosis of the ecological status of the Guadalquivir estuary in the light of proposing remediation management actions to recover the ecosystem-services supplied by this environment (Ruiz et al. 2017).

Methods

Study area

The Guadalquivir river is one of the longest fluvial courses in Spain with a total length of 680 km that extends from its source in the Cazorla mountains, approximately 1400 m above sea level, to its mouth at Sanlucar de Barrameda in the Gulf of Cadiz (Fig. 1). The estuary occupies the river´s last 110 km, hosting a population of 1.7 million people that are clustered in large municipalities that rely on the estuary to support different socioeconomic sectors (agriculture, fisheries, tourism) (Ruiz et al. 2015). As a mesotidal

Fig. 1 Location of the Guadalquivir estuary. Sampling stations are indicated by the red dots (Color figure online)

system, tidal influence can be noticeable up to 100 km upstream of the river mouth, where a dam is located (Díez-Minguito et al. 2012). Because the climate in the catchment area (63,822 km^2) is Mediterranean sub-humid with well defined seasonality, freshwater discharges from the dam exhibit marked seasonal variations in magnitude and duration. During the dry periods (70% of the hydrological year) discharges lower than 40 $m^3\ s^{-1}$ regularly occur, which are nevertheless sufficient to compensate evaporation losses. These conditions are normal for this estuary (Díez-Minguito et al. 2012). During the wet season (usually lasting from October to April) that is usually characterized by relatively short but intense periods of rainfall, freshwater inputs into the estuary may yield levels exceeding 400 $m^3\ s^{-1}$, which interferes with the tidal effect and disrupts tidal dominance (Díez-Minguito et al. 2013). In fact, high to very high discharges (ranging from 500 to 1000 $m^3\ s^{-1}$) induce a regime shift due to the high-suspended sediment concentrations brought by the freshwater inputs (Losada et al. 2017). Elevated concentrations of suspended matter are also found under normal conditions, although several orders of magnitude lower than those under periods of high discharges (Losada et al. 2017). The estuary is heavily dredged on a regular basis to deepen the navigation channel and ensure access for large container ships to the port of Sevilla, which delivers high load of inorganic compounds to the water column (Caballero et al. 2018).

Sampling strategy

Samples were taken at five sites (Fig. 1) during eight cruises conducted between March 2016 and March 2017 using a 4.85 m inflatable boat. Sampling dates and monthly environmental conditions are listed in Table 1. All surveys commenced at the mouth of the estuary during spring and rising tide. This strategy may have had implications for gas distribution, as sampling went along with the net saltwater flux into the system and salinity could affect the concentration gradient. However, being aware of this caveat, the sampling design ensured comparable mixing conditions every month and also allowed minimizing survey duration.

From site 1 positioned at the river mouth, sites 2, 3 and 4 were located at 10, 15 and 20 km upstream, respectively. Site 5, at 25 km from the river mouth, represented the entry of the estuary into a creek that penetrates the saltmarshes of Doñana National Park, the largest coastal wetland of South

Table 1 Relevant physico-chemical characteristics of the Guadalquivir estuary during the sampling period

Sampling date	Water temperature (°C)	Monthly wind speed (ms^{-1})	Salinity range sampled	Tidal[a] coefficient	Montly discharge ($m^3\ s^{-1}$)	Montly rainfall (mm)
18 March 2016	15.4 ± 0.2	2.36	8–28	56	14	22
21 April 2016	18.4 ± 0.6	2.93	3–26	84	27	70
19 May 2016	22.1 ± 1.3	3.05	0.5–9	74	47	153
14 Nov 2016	17.3 ± 0.1	2.11	12–33	111	46	144
13 Dec 2016	14.9 ± 0.2	1.83	2–18	103	44	85
20 Jan 2017	9.5 ± 1.1	1.74	3–17	41	15	25
7 Feb 2017	12.8 ± 0.2	2.26	4–19	70	28	55
24 March 2017	15.8 ± 0.3	2.43	7–25	67	43	82

[a]Difference in height between the consecutive high tides and low tides in the area

Europe. This site was chosen to assess the environmental status of estuarine waters feeding the southern sector of the Park, which had been isolated from the estuary until very recently (Huertas et al. 2017a). At each site, conductivity, temperature and pH were obtained with a Yellow Spring (YSI Incorporate) portable multiparameter probe YS6820v2. Discrete water samples were taken with a Niskin bottle at 1 m depth to determine CH_4 and N_2O concentrations, inorganic nutrients (NH_4^+, NO_2^-, NO_3^-, PO_4^{3-}, and Si), DO, total dissolved nitrogen (TDN), dissolved organic carbon (DOC), suspended particulate matter (TSM) and chlorophyll (Chl *a*). The Guadalquivir estuary is classified as totally mixed mesotidal (de la Paz et al. 2007; Ruiz et al. 2017) and thus, 1 m depth samples were assumed to be representative for the entire water column.

Analytical techniques

Samples for N_2O and CH_4 were collected in duplicate 120 mL serum vials, sealed and preserved with $HgCl_2$ to inhibit microbial activity. Trace gas samples were stored upside down in the dark until analysis in the laboratory by static-head space equilibration gas chromatography (GC) using an Agilent 7890 GC equipped with an Electron Capture Detector (ECD) for N_2O and Flame Ionization Detector (FID) for CH_4 as described in de la Paz et al. (2015). Before chromatographic determination, 20 mL of N_2 headspace were introduced in each sample and equilibrated for at least 12 h after initial vigorous shaking. The GC system was calibrated using three standard gas mixtures of different origin: a certified NOAA primary standard with composition similar to the atmosphere (324.97 ± 0.13 ppb for N_2O and 1863.4 ± 0.3 ppb for CH_4), and two additional standard gas mixtures of N_2O and CH_4 in a N_2 matrix provided by Air Liquide (France) with certified concentrations (1020 and 3000 ppb for N_2O; 3000 and 5000 ppb for CH_4). The precision of the method estimated from the coefficient of variation based on replicate analysis was 0.6% for CH_4 and 0.4% for N_2O. Saturation values expressed as percentage (%) for CH_4 and N_2O were computed as the ratio between the gas concentration measured and the calculated equilibrium concentration for both gases. Calculations of the equilibrium concentrations in the water phase were done using the annual averaged atmospheric mixing ratios CH_4 ($\times CH_{4atm}$) and N_2O ($\times N_2O_{atm}$) provided by the World Data Center for Greenhouse Gases (http://ds.data.jma.go.jp/gmd/wdcgg/) due to lack of data during the study period in the nearest station of the global monitoring network. Such mean values were calculated as 1866 and 328 ppb for $\times CH_{4atm}$ and $\times N_2O_{atm}$ respectively.

Water samples (5 mL, two replicates) for nutrient analyses were filtered immediately (Whatman GF/F, 0.7 µm), and stored frozen (− 20 °C) for later analyses in the shore-based laboratory. Dissolved nitrate, nitrite and ammonium concentrations were measured with a continuous flow auto analyzer (SkalarSan + + 215) using standard colorimetric techniques (Hansen and Koroleff 1999). Analytical precisions were always better than ± 3%.

DO concentrations were fixed immediately and measured within 24 h upon collection in sealed flasks stored in the dark through an automated potentiometric modification of the original Winkler method using a Metrohm 794 Titroprocessor, with an estimated error of ± 5 µmol kg^{-1}.The saturation values of O_2 were calculated with the equation given by Benson and Krause (1984) and the apparent oxygen utilization (AOU) was obtained by subtracting the oxygen concentration at saturation to the observed oxygen concentration.

Total alkalinity (TA) was also determined by titration of samples collected in borosilicate bottles (500 mL) and poisoned with 100 µL of a $HgCl_2$ saturated aqueous solution, according to Mintrop et al. (2000). Accuracy (± 5 µmol kg^{-1}) was obtained from regular measurements of Certificate Reference Material supplied by Prof. Andrew Dickson, Scripps Institution of Oceanography, La Jolla, CA, USA (Batch #147). Partial pressure of CO_2 in water (pCO_2) was computed from TA and pH_{NBS} pairs through the CO2SYS.

xls program (Lewis et al. 1998) using the Cai and Wang (1998) and Dickson (1990) constants for carbon and sulfate, respectively.

Concentrations of DOC and TDN were determined by catalytic oxidation at high temperature (720 °C) and chemiluminescence, respectively in a Shimadzu Total Organic Carbon analyzer (Model TOC-$V_{CPH/CPN}$), according to Álvarez-Salgado and Miller (1998). Analytical precision of the methods was always better than 0.015 and 0.03 mg L^{-1} for DOC and TDN measurements respectively.

TSM, particulate organic and inorganic matter (POM and PIM respectively) were determined by the loss on ignition (LOI) method. Known volumes of water were filtered (precombusted 450 °C Whatman GF/F, 0.7 µm) and filters dried at 60 °C for 48 h. They were subsequently weighed to derive TSM (g L^{-1}), further combusted again at 450 °C for 5 h, and weighed to derive PIM and POM by difference.

Chl *a* analysis was conducted by filtering known volumes of water (Whatman GF/F, 0.7 µm) and filters were dipped in 90% acetone overnight in the dark for extraction. Pigment concentrations were obtained by fluorometry with a Turner Designs 10-AU Model fluorometer, which was calibrated using a pure Chl *a* standard from the cyanobacterium *Anacystis nidulans* (Sigma Chemical Company). The precision of the method was 0.025 µg L^{-1}.

Air–water gas exchange

The gas flux (F, µmol m^{-2} day^{-1}) between the atmosphere and estuarine waters was calculated as:

$$F = k\,(C_w - C_a), \quad (1)$$

where k (cm h^{-1}) is the gas transfer rate as a function of wind speed at 10 m height, C_w is the measured dissolved gas concentration, and C_a is the equilibrium concentration in water based on the molar atmospheric ratio as above. k was computed from k normalized to a Schmidt number of 600 (k_{600}) according to:

$$k = k_{600}\sqrt{\frac{600}{Sc}},$$

where Sc is the Schmidt number of each gas calculated from water temperature with the formulations given by Wanninkhof (1992), which has been widely applied and facilitates comparison with other systems.

k_{600} was computed from U_{10} using the parameterization given by Jiang et al. (2008).

$$k_{600} = 0.314 \times U_{10}{}^2 - 0.436 \times U_{10} + 3.99,$$

where U_{10} was calculated according to Smith (1988) using monthly averaged wind speed data provided by a nearby automatic meteorological station located in Lebrija (36°58×35″N, 06°07×34″W) from the Junta de Andalucía network (http://www.juntadeandalucia.es/agriculturaypesca/ifapa/ria/servlet/FrontController).

There is no current consensus about the best parameterization of the gas transfer rate to be used for computation of the air–water gas exchange in estuaries. We chose the wind-dependent expression provided by Jiang et al. (2008) that has been formulated specifically for estuaries by refitting the data compiled by Raymond and Cole (2001) with newer gas exchange measurements in estuaries.

Daily discharge data from the Alcala del Rio dam and rainfall from the Lebrija station were obtained from the Sistema Automático de Información Hidrológica for the Guadalquivir basin (http://www.chguadalquivir.es/saih/Inicio.aspx).

All data contained in this work are available for download from Digital.CSIC, the Institutional Repository of the Spanish National Research Council (CSIC), (https://digital.csic.es/handle/10261/160022, https://doi.org/10.20350/digitalCSIC/8528).

Statistics

Statistics were performed with the program language MATLAB. Probability distributions of variables were examined through a Shapiro–Wilk test. Pearson's product-moment correlation (PPMC) was used to test for significant correlations between variables. Significance levels were set at $p < 0.05$. When normality was not met, the criterion established by Havlicek and Peterson (1977) was applied.

Results

Dynamics of CH_4 and N_2O in the estuary

During the sampling period, CH_4 and N_2O concentrations ranged from 14 to 750 nmol L^{-1} and from 3 to 34 nmol L^{-1}, respectively (Table 2). As a general trend, an increase in the average concentration of both gases was observed upstream, with CH_4 mean values of 27 and 167 nmol L^{-1} at sites 1 and 5 respectively and N_2O mean values of 15 and

Table 2 Average concentrations (±SD) of dissolved CH_4 and N_2O and concentration ranges in the sites chosen at the Guadalquivir estuary during the sampling period

Site	CH_4 (nmol L^{-1})	CH_4 range (nmol L^{-1})	N_2O (nmol L^{-1})	N_2O range (nmol L^{-1})
1	27.5 ± 9	16–39	15.8 ± 5	9–25
2	36.2 ± 5	28–42	17.9 ± 5	10–26
3	38.7 ± 5	34–50	20.2 ± 7	11–29
4	36 ± 15	14–61	20 ± 7	12–34
5	167.7 ± 244	38–750	17.4 ± 7	3–29

17 nmol L^{-1} in the same sites (Table 2). Methane levels in the lowest saline samples ranged from 14 to 750 nmol L^{-1} whereas concentrations at the highest salinities ranged from 16 to 39 nmol L^{-1} (Table 3). In the case of nitrous oxide, concentrations in the samples characterized by the lowest salinities varied from 3 to 29 nmol L^{-1}, which were similar to those found in samples with the highest salinities and that ranged between 9 and 25 nmol L^{-1} (Table 3). For both gases, concentration in freshwater samples exhibited a higher variability than in their marine counterparts, which was particularly evident in the case of methane (Table 3).

The salinity range found within the estuary transect during the different surveys also exhibited marked variations (Table 1). The spatio-temporal variability of salinity (Fig. 2) seemed to be related to the tidal amplitude (Table 1). Thus, during periods of maximum rainfall (May and November 2016), higher discharges from the dam occurred (> 45 m^3 s^{-1}, Table 1) and even though the magnitude of the freshwater inputs was equivalent, the salinity gradient in the water course clearly differed between both months (Table 1). In May, a sharp decline in salinity was observed in all sites, dropping to nearly 0, except in the site located closer to the river mouth (site 1), where salinity reached approximately 10 (Fig. 2). In contrast, in November, salinity approached seawater values at sites 1 and 2, also increasing upstream in relation to other months (Fig. 2), which can be attributed to the tidal coefficient (or amplitude of the tide forecast) present at spring tide that was the highest for the entire sampling period (Table 1). The remaining samplings were characterized by slight variations in salinity in each site, although a clear salinity gradient throughout the estuary transect was still detected (Fig. 2). Noticeable changes in the concentration of biogeochemical variables occurred during May and November 2016 in relation to other surveys. The rise in freshwater flow along the estuary in May was accompanied by a decrease in DO levels (particularly in site 5) and increases in the concentrations of DOC, TDN (except in site 5), CH_4 and N_2O, although a marked reduction in nitrous oxide was observed in site 5 that even declined below saturation (Fig. 2). The drop of N_2O in the tidal creek coincided with the highest concentration of methane measured during the sampling period (Fig. 2). In contrast, when the tide propagated further upstream during November 2016, as indicated by the rise in salinity in all sites (Fig. 2), DOC, TDN and N_2O decreased along the estuary whereas methane concentration increased in sites 2, 3 and 4 and decreased in sites 1 and 5.

Fig. 2 Temporal variation of salinity and concentration of dissolved oxygen, organic carbon, total nitrogen, CH_4 and N_2O (open symbols) at the five sites sampled along the Guadalquivir estuary during eight surveys conducted between March 2016 and March 2017. Note that Y axis scale for several parameters varies for site 5

Sources of CH_4 and N_2O

Table 4 summarizes the results of the Pearson correlations performed with the complete dataset of the variables measured. Methane concentration was shown to be positively and significantly ($p < 0.05$) correlated with Chl *a*, DOC, AOU and pCO_2 and inversely correlated with N_2O and nitrate. Accordingly, nitrous oxide concentration was significantly ($p < 0.05$) and directly correlated with NO_3^- and negatively correlated with salinity. Furthermore, strong and significant relationships were found between pCO_2, DOC and AOU, indicating that organic matter degradation played an important role in generation of carbon dioxide within the estuary, which ranged between 522 and 4300 ppm and increased as salinity decreased (Fig. 3 and note the negative and significant correlation between pCO_2 and salinity in Table 4). Salinity also correlated quite well with Chl *a* concentration and DOC (Table 4; Fig. 3), suggesting that the spatial distribution of these biogeochemical variables was governed by the mixing between freshwater and oceanic water. Nevertheless, a higher variability in the concentration of both variables was observed in riverine waters (salinity < 10) in relation to the levels found in saltier waters (Fig. 3), as was observed for CH_4 and N_2O concentrations (Table 3). The relationship between the levels of both gases in the estuary and salinity was illustrated by plotting the percentage of saturation of dissolved CH_4 and N_2O as a function of salinity (Fig. 4a).

Table 3 Summary of the concentration of methane and nitrous oxide found in samples with the smallest and highest salinity in the Guadalquivir estuary during each survey

Survey	Salinity	CH_4 (nmol L^{-1})	N_2O (nmol L^{-1})	Salinity	CH_4 (nmol L^{-1})	N_2O (nmol L^{-1})
March 16	8	38	21	28	23	16
April 16	3	14	13	26	18	13
May 16	0.5	750	3	9	39	25
Nov. 16	12	56	13	33	16	9
Dec. 16	2	50	29	18	39	21
Jan. 17	3	227	22	17	29	15
Feb. 17	4	42	18	19	33	15
March 17	7	42	16	25	22	13

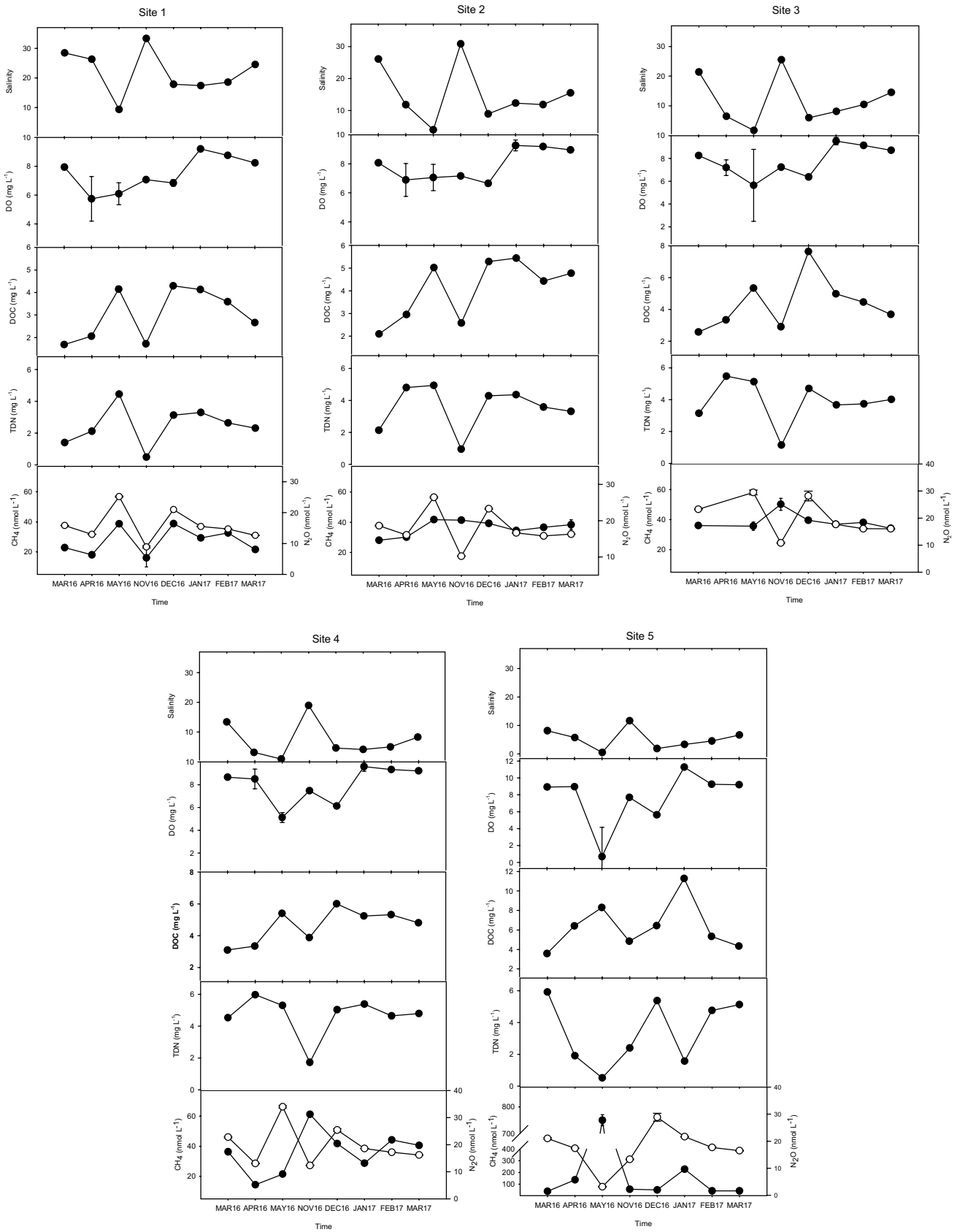
Site 1
Site 2
Site 3
Site 4
Site 5
Salinity
DO (mg L⁻¹)
DOC (mg L⁻¹)
TDN (mg L⁻¹)
CH4 (nmol L⁻¹)
N2O (nmol L⁻¹)
MAR16 APR16 MAY16 NOV16 DEC16 JAN17 FEB17 MAR17
Time

Table 4 Pearson correlation matrix for biogeochemical variables measured in the Guadalquivir estuary

CH_4	N_2O	Salinity	Temp.	Chi *a*	TSM	DOC	TDN	NH_4^+	NO_2^-	PO_4^{3-}	NO_3^-	AOU	pCO_2
CH_4	− 0.35*	− 0.29	0.30	0.42*	− 0.09	0.52*	− 0.38*	− 0.22	0.02	0.24	− 0.40*	0.63*	0.53*
N_2O		− 0.48*	0.02	0.11	− 0.03	0.30	0.64*	− 0.28	0.08	0.27	0.61*	0.18	0.23
Salinity			− 0.06	− 0.41*	0.39*	− 0.72*	− 0.67*	0.82*	0.05	− 0.59*	− 0.58*	− 0.44*	− 0.52*
Temp.				0.04	0.38*	− 0.18	− 0.05	− 0.08	0.31	0.50*	0.15	0.43*	0.24
Chi *a*					− 0.24	0.68*	− 0.16	− 0.45*	0.58*	− 0.21	− 0.13	-0.03	0.13
TSM						− 0.42*	− 0.29	0.53*	0.01	-0.02	− 0.21	0.14	− 0.12
DOC							0.12	− 0.59*	0.14	0.22	− 0.02	0.44*	0.61*
TDN								− 0.55*	− 0.25	0.48*	0.94*	0.07*	0.09
NH_4^+									− 0.05	− 0.37*	− 0.49*	− 0.23	− 0.27
NO_2^-										− 0.32	− 0.13	− 0.16	− 0.17
PO_4^{3-}											0.50*	0.66*	0.61*
NO_3^-												0.03	0.04
AOU													0.79*

The values were established with the complete dataset obtained during all the sampling campaigns. Abbreviations are indicated in the text

*Correlations significant at $p < 0.05$

Estuarine waters were always over-saturated in methane and nitrous oxide with respect to the atmospheric equilibrium, with the exception of site 5 in which N_2O under-saturation (39%) in relation to the atmospheric N_2O level was found in May 2016 at a very low salinity (0.5, Table 3; Fig. 4a). With the exception of that finding, higher N_2O over-saturations were measured in the freshwater portion of the estuary (salinity < 10) regardless of the sampling month, with the highest value approaching 400% in May 2016. Hence, a gradual decreasing gradient of N_2O saturation with salinity was noticeable, which was especially evident in the surveys conducted in May and December 2016. This pattern was not so clear for methane, which exhibited an oversaturation range between 520 and 30,800%, and even though higher values were observed in the freshwater–saltwater interface a more scattered distribution was found (Fig. 4a).

In order to gain insights on the effect of ecosystem metabolism on the dynamics of CH_4 and N_2O within the estuary, the relationship between the trace gas saturation levels and the oxygen availability was also examined. It is worth noting that the N_2O outlier measured in site 5 during May 16 (39% N_2O saturation at $\%O_2$ saturation of 14) was not statistically considered. As shown in Fig. 4b, $\log_{10}$ $\%CH_4$ vs. $\%O_2$ displayed a weak but significant negative relationship ($r^2 = 0.33$, $n = 40$) whereas $\%N_2O$ was strongly and negatively related with $\%O_2$ (Fig. 4b; $r^2 = 0.56$, $n = 40$) (Fig. 5).

CH_4 and N_2O emission fluxes

CH_4 emissions varied from ~ 13 µmol m^{-2} day^{-1} in site 1 in November 2016 to a maximum of nearly 1100 µmol m^{-2} day^{-1} at site 5 in May 2016, although no clear seasonal variation in CH_4 fluxes could be detected (Fig. 5). A tendency to higher methane effluxes was observed upstream regardless of the sampling month, although emissions remained below 50 µmol m^{-2} day^{-1} in most sites with the exception of site 5 in which the outgassing markedly increased in April and May 2016 and January 2017.

N_2O emissions from the estuarine transect were higher in May 2016 (Fig. 5) coinciding with the flushing of the estuary with freshwater (Fig. 2; Table 1), although during this month, site 5 displayed the only negative N_2O flux measured during the whole sampling period and equivalent to − 7.1 µmol m^{-2} day^{-1}. Overall, downstream sites exhibited lower N_2O emissions, with the lowest N_2O effluxes (below 4 µmol m^{-2} day^{-1}) occurring in all sites in November 2016, when the estuary experienced the highest tidal intrusion (Fig. 2; Table 1).

Discussion

Sources of CH_4 and N_2O in the Guadalquivir estuary

The spatio-temporal distribution of dissolved CH_4 and N_2O in the Guadalquivir estuary reflects the hydrodynamics of the system, in which tidal-fluvial interaction is a major driver of the ecosystem metabolic status (Losada et al. 2017; Ruiz et al. 2017). The associations found between the salinity gradient and Chl *a*, DOC, and pCO_2 within the estuary are in agreement with previous findings indicating that the patterns of primary production, organic matter degradation and CO_2 emissions are tightly coupled to the freshwater discharge/tidal regime (Flecha et al. 2015; Ruiz et al. 2017). Our study now reveals that the levels of CH_4 and N_2O observed in the Guadalquivir estuary are also closely related to the balance

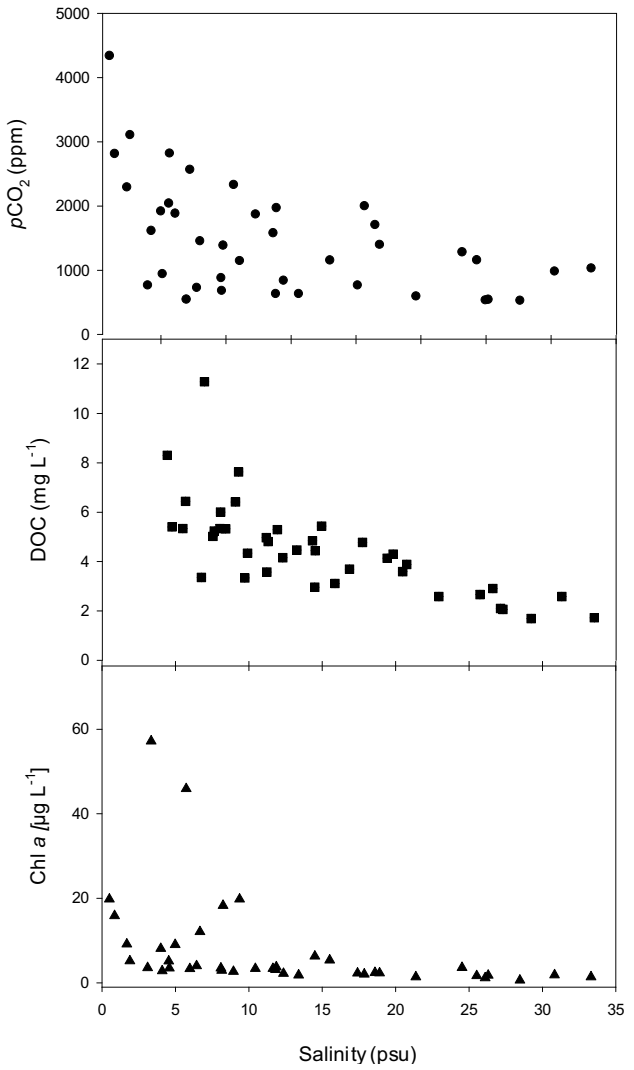

Fig. 3 Dissolved carbon dioxide (pCO_2), dissolved organic carbon (DOC) and Chlorophyll (Chl *a*) vs. salinity in the estuary transect

between the intrusion of the saline plume and the magnitude of freshwater inputs. Even though this relationship was seen along the entire estuarine transect, it was especially noticeable in the tidal creek where levels of CH_4 and N_2O markedly varied in response to drastic changes in salinity (for instance May and November 2016). The effect of the tidal-fluvial interaction on the trace gas distributions in the estuary could proceed either in a direct way (e.g. sulfate inhibition on methanogenesis) or indirectly through the influence of hydrodynamics on the biogeochemistry of the water course (e.g. changes in nutrient supply or oxygen availability). The average CH_4 concentration and over-saturations measured in the Guadalquivir estuary fall in the lower portion of the range reported for temperate and tropical estuaries and rivers (Koné et al. 2010; Maher et al. 2015; Middelburg et al. 2002; Sansone et al. 1999; Shalini et al. 2006; Smith et al. 2000; Upstill-Goddard and Barnes 2016; Upstill-Goddard et al. 2017; Zhang et al. 2008). In addition, no clear seasonal signals in methane levels could be discerned, contrary to what has been observed in other fluvial catchments and estuaries (Bouillon et al. 2012; Koné et al. 2010; Middelburg et al. 2002; Shalini et al. 2006; Upstill-Goddard et al. 2017). This is probably the result of several processes influencing water column CH_4, as methane in estuaries stems from several sources: (1) microbial production in sediments that fluxes to the water column, (2) microbial production in adjacent wetlands and transport by the river, or (3) in situ microbial CH_4 production as a result of anaerobic organic matter decomposition. The interaction of these pathways with seasonal signals in estuarine hydrodynamics may mask any seasonality in biogeochemistry due to the effect of temperature alone, as suggested for other European estuaries (Upstill-Goddard and Barnes 2016).

Furthermore, it is understood that moderate to high salinity aquatic systems typically show much lower surface water methane concentrations and emissions than freshwater habitats. This is partially due to the high concentration of sulfate in seawater that allows sulfate-reducing bacteria to outcompete methanogenic bacteria for energy sources, consequently inhibiting methane production (Bartlett et al. 1987; Borges and Abril 2011). However, the association between salinity and methane formation can be complicated by site-specific conditions and methane can be also produced in saline environments despite the inhibitory effects of sulfate (Borges and Abril 2011). A compilation of methane measurements in 31 temperate tidal marshes revealed an inverse log-linear relationship between salinity and methane emissions (Poffenbarger et al. 2011). This study concluded that the range of methane emissions from saline marshes could be predicted by salinity and those systems characterized by salinity > 18 have negligible methane production. In our work, methane distribution and effluxes along the Guadalquivir estuary suggest that even though salinity was not the primary controlling factor for methane generation, sulfate inhibition must have been proceeding, as higher CH_4 oversaturations were measured at riverine waters. Additionally, gas concentrations in samples characterized by the lowest salinities were much higher than those in their marine counterparts. Hence, the magnitude of the tidal intrusion likely affected methane distribution in the estuary.

In addition to the sulfate inhibition of CH_4 formation, the decrease of CH_4 concentration with salinity could be due to gas loss terms, such as microbial oxidation and emission to the atmosphere. Dissolved methane loss by these processes can be very fast in coastal and estuarine environments, as recently found by Borges et al. (2017) in the southern bight of the North Sea.

Our results also indicate that anaerobic matter degradation in the water column during the sampling period was

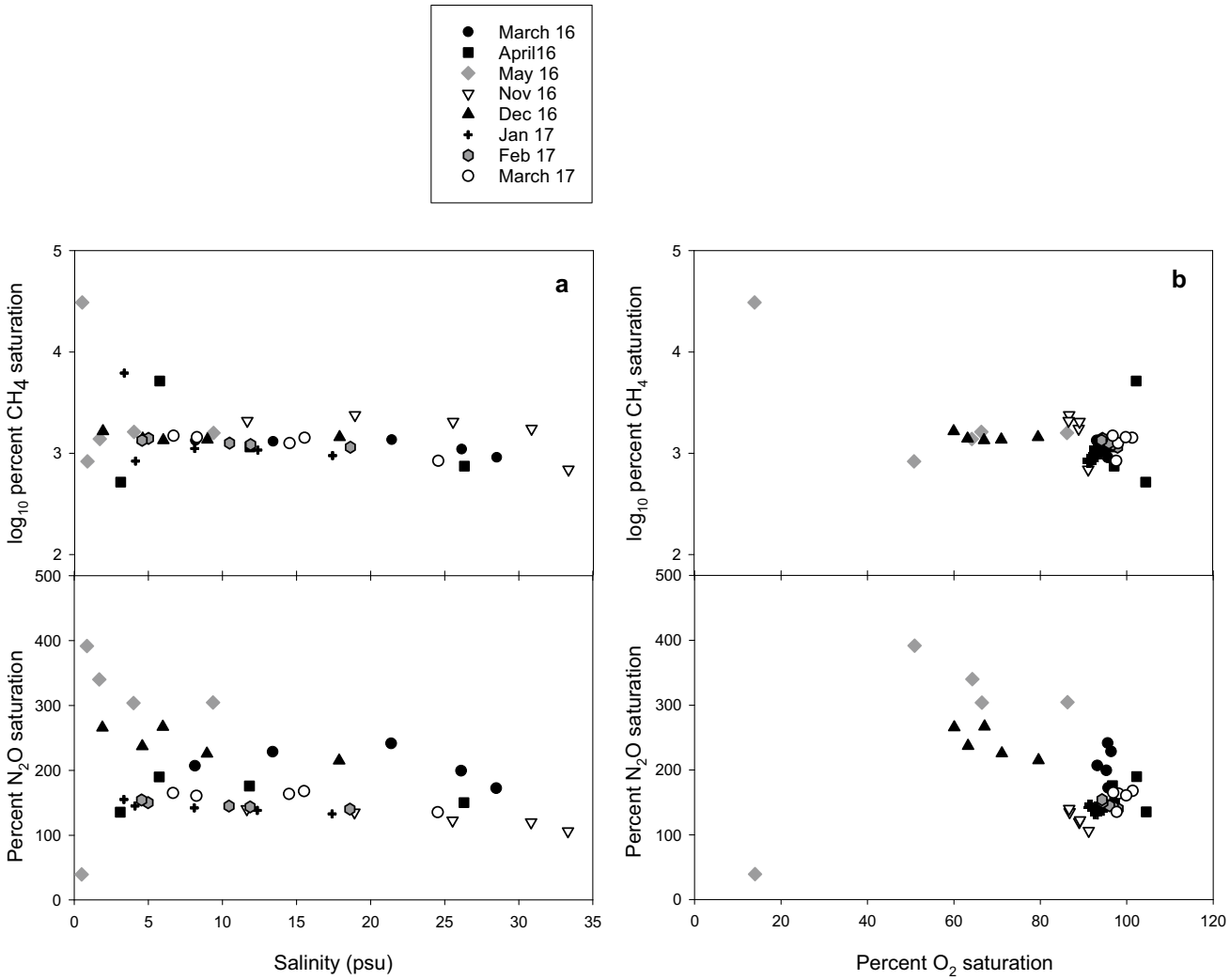

Fig. 4 **a** $\log_{10}$ percent dissolved methane saturation ($\log_{10}\%CH_4$) vs. salinity (upper panel) and percent dissolved nitrous oxide saturation ($\%N_2O$) vs. salinity (lower panel) and **b** $\log_{10}$ percent dissolved methane saturation vs. percent dissolved O_2 saturation ($\%O_2$) (upper panel) and percent dissolved nitrous oxide saturation vs. percent dissolved O_2 saturation (lower panel) for the Guadalquivir estuary

unlikely, as even though DO was undersaturated most of the time, oxygen concentrations remained above 5 mg L^{-1}. Under these aerobic conditions, CH_4 levels were still moderate, with saturations ranging from ~520 to 6000%. Therefore, methane diffusion from the sediment was probably the major source of CH_4 to the water column. However, it is notable that when an event of isolated hypoxia occurred at site 5 during May 2016 (0.69 mg L^{-1}, corresponding to O_2 undersaturation of 14%), methane concentration sharply increased to reach nearly 800 nmol L^{-1} (over saturation of 30,000%), which could suggest in situ aquatic microbial CH_4 production by anaerobic organic matter degradation. Nevertheless, methanogens are sensitive to low oxygen concentrations and are slow growing organisms unlikely to proliferate in the water column on short time-scales (Bridgham et al. 2013). Moreover, even though there is circumstantial evidence for CH_4 production in the water column, it proceeds under very stable conditions, for instance, in stratified oligotrophic lakes (Grossart et al. 2011). Hence, the most plausible explanation for the high CH_4 concentration is that methane losses via microbial oxidation would have been minimized, which would result in the local massive efflux detected. This association between methane release in response to dissolved oxygen decay has been found in some African streams (Borges et al. 2015b). This finding may be particularly relevant for methane emission patterns in the Guadalquivir estuary, where prolonged episodes of hypoxia have been observed after the entry of considerable suspended matter loads by high freshwater discharges (Flecha et al. 2015; Ruiz et al. 2015, 2017). The relationship found between $\log_{10}\%CH_4$ vs. $\%O_2$ indicates that when oxygen saturation dropped below 15%, the level of dissolved methane

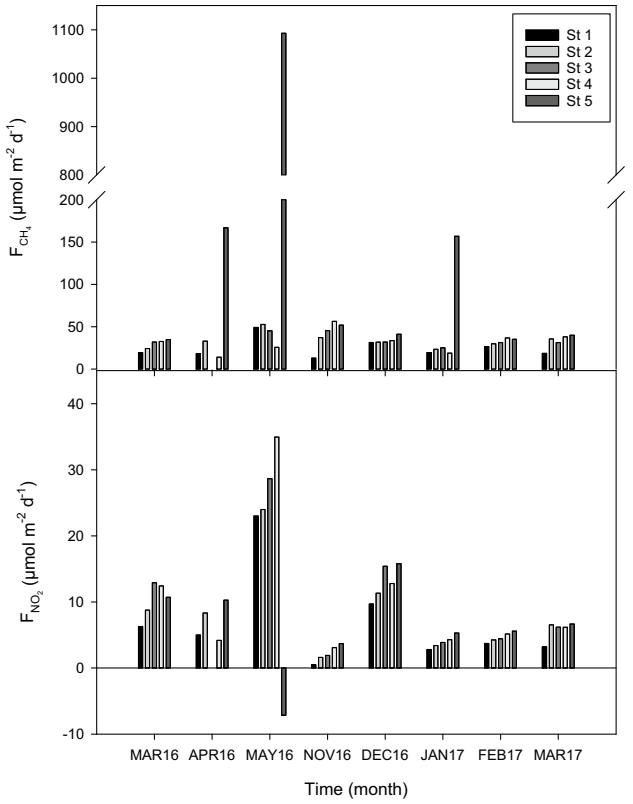

Fig. 5 Temporal variation of the air–water CH_4 (upper panel) and N_2O (lower panel) fluxes for the Guadalquivir estuary during the eight surveys conducted between March 2016 and March 2017

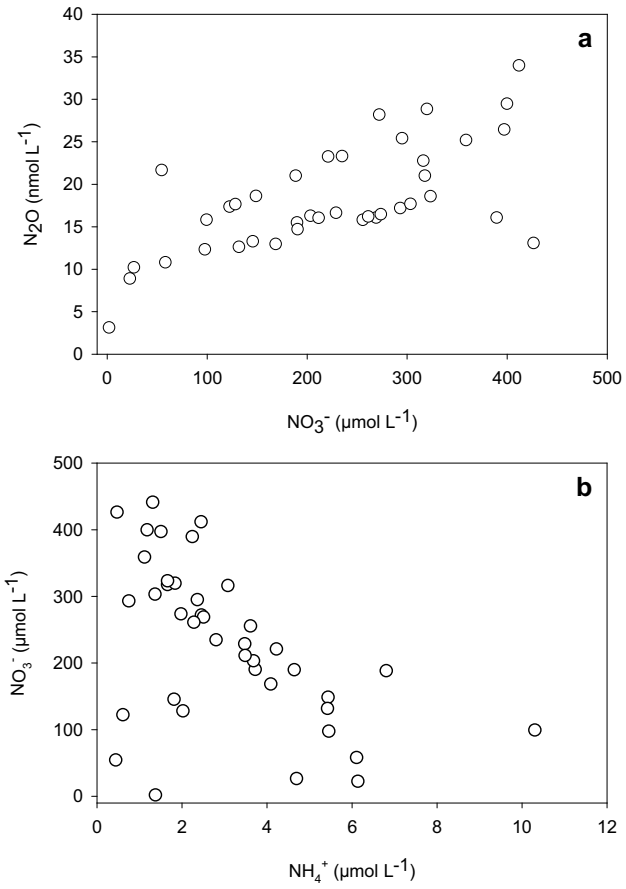

Fig. 6 **a** Dissolved nitrous oxide concentration vs. nitrate and **b** dissolved nitrate vs. dissolved ammonium for the Guadalquivir estuary

sharply rose. Therefore, a rise in methane accumulation may be expected in the estuary under high freshwater flooding events, which are common during rainy seasons wetter than that of our study (Losada et al. 2017), as they increase turbidity, reduce sulfate inhibition and cause hypoxia.

It should be noted that freshwater inputs do not necessarily always lead to higher CH_4 levels. For instance, in the Meuse river network the highest fluvial methane concentrations have been found during low water due to gas accumulation favored by the increase in residence time and temperature (Borges et al. 2018). Our data suggest that in the case of the Guadalquivir estuary high freshwater is more likely to result in CH_4 accumulation due to its effect on the aforementioned mechanisms.

During our sampling period, no correlation between CH_4 concentration and turbidity (represented by the TSM content) was found, contrary to the trend reported in some British estuaries (Upstill-Goddard et al. 2000). However, this feature does not preclude that such association could occur in the estuary during episodes of greater turbidity (Losada et al. 2017).

Periods characterized by a high DOC content but aerobic conditions, such as those in April 2016 and January 2017 in the creek (site 5) coincided with increased methane levels (~ 200 nmol L^{-1}). This suggests contribution of lateral inputs from the adjacent Doñana marshes, which are significant CH_4 emitters (Huertas et al. 2017b). In the main channel of the estuary, methane was also significantly and positively correlated with DOC and Chl*a*. As both variables represent the balance between respiration and productivity in aquatic ecosystems, the direct relationships found with CH_4 indicate that methane dynamics in the estuary are regulated by a combination of complex biological interactions. The tight couplings between pCO_2, CH_4, DOC, PO_4^{3-} and AOU suggest that the dynamics of pCO_2, CH_4 and DO were driven by net heterotrophy, as described in freshwater systems (Borges et al. 2015a; Lapierre and del Giorgio 2012) and tidal estuaries (Maher et al. 2015).

Despite methanogenesis being carried out by severely O_2-limited archaea (Bridgham et al. 2013), the existence of high CH_4 concentrations in oxygenated aquatic systems, as occurred in the Guadalquivir estuary during our study period, is a well known phenomenon. Diffusion of the methane produced in the anoxic sediments and inputs from

adjacent floodplain soils and wetlands may have contributed to such pattern, but also methanogenesis in anoxic microsites present in oxygenated soils, which is even activated during flooding (Bridgham et al. 2013; Von Fischer and Hedin 2007). Methane production by photoautotroph-attached archaea (Grossart et al. 2011), and non-microbial aerobic formation in plant tissues (Keppler et al. 2006, 2009) and soils (Hurkuck et al. 2012) have also been reported. Therefore, some of these processes or a combination of them, may have been active in the Guadalquivir estuary during our surveys. Clearly, further work is needed to identify the methane production pathways in the river and their control by environmental factors.

Nitrate availability could also play a role by suppressing methanogenesis (Klüber and Conrad 1998), which has been described recently in some streams of North America (Schade et al. 2016). The negative correlation between CH_4 and NO_3^- would fit the conceptual model of Schade et al. (2016). Nevertheless, the influence of nitrate on CH_4 dynamics was not clearly identified in a global meta-analysis of riverine CH_4 conducted by Stanley et al. (2016), who stated that the dual role of NO_3^- as both nutrient and transport electron acceptor complicates the assessment of the relationship between methane and nitrogen availability. In a recent work, Borges et al. (2018) did not find any significant correlation between CH_4 and NO_3^- in the Meuse river network. As indicated by these authors, it is uncertain if correlations between these variables are the result of a direct causality or due to a common driver, such as oxygen availability in the case of the Guadalquivir estuary. Moreover, in mesotidal systems, the inhibitory effect of sulfate on methanogenesis must also be incorporated into the regulation pathways and hence, no definitive conclusion on the regulatory effect of nitrate on CH_4 dynamics can be drawn from our data set.

N_2O cycling in estuaries is also regulated by complex processes involving oxygen availability, nitrogen load, organic matter inputs, groundwater, and mixing (Codispoti 2010; Murray et al. 2015). Our data reveal a connection between N_2O levels and the magnitude of freshwater inputs within the estuary. The downstream sites 1 and 2 always exhibited lower N_2O concentrations, which also decreased in the whole estuarine transect during the tidal intrusion in November 2016. However, the $\%N_2O$ vs. salinity plot suggests that dilution alone cannot explain N_2O distribution. In fact, the influence of the fluvial-tidal interaction on N_2O estuarine levels seemed to occur through the effect of mixing on the nitrogen concentration since when dissolved nitrogen compounds fell as the result of the tidal flushing, N_2O concentrations invariably dropped. Therefore, nitrogen loading within the estuary that is heavily regulated by the mixing conditions may be claimed as a major driver of N_2O generation patterns in the system.

This association between N_2O and the nitrogen content but especially with NO_3^- points towards nitrification as the main N_2O formation pathway. Parallel increases in NO_3^- and N_2O, which were found in our data set (Fig. 6a), are an indication of nitrification (Beaulieu et al. 2010; Silvennoinen et al. 2008). Furthermore, NO_3^- that was the main form of inorganic nitrogen in the estuary, also rose as NH_4^+ concentrations decreased (Fig. 6b), providing additional evidence for N_2O produced during nitrification. Nitrification-derived N_2O has been described in the Schelde estuary (Wilde and de Bie 2000), some British estuaries (Barnes and Upstill-Goddard 2011) and in the Elbe estuary (Brase et al. 2017). The relationship found between $\%N_2O$ vs. $\%O_2$ supports our conclusion on the prevalence of nitrification in the Guadalquivir estuary. The lowest N_2O value (below atmospheric equilibrium) of the data series observed at site 5 in May 2016 concurred with the isolated event of hypoxia and the highest pCO_2 level registered (~4330 ppm), conditions that were not observed in the rest of surveys, which together suggests removal of nitrous oxide by denitrification. This observation is in agreement with patterns described in the Amazon floodplains (Richey et al. 1988) and in some African rivers (Borges et al. 2015b) and is relevant for N_2O dynamics in an ecosystem where prolonged hypoxic episodes have been reported (Ruiz et al. 2015).

In comparison to other European estuaries, N_2O concentrations and saturation levels in the Guadalquivir estuary are in the mid range of values reported. The mean N_2O saturation of 183% (±69%) in the estuary is comparable to those measured in the Gironde (Bange 2006), Temmesjoki (Silvennoinen et al. 2008), Tagus (Gonçalves et al. 2010) and Elbe (Brase et al. 2017) estuaries but lower compared to the Schelde (*de* Bie et al. 2002) and below the overall value estimated for European estuaries (Barnes and Upstill-Goddard 2011).

CH_4 and N_2O emissions

The mean CH_4 flux during our sampling period was 66.20 (±171) μmol m^{-2} day^{-1}, which falls within the range of air–water CH_4 exchange reported in temperate rivers from 0 to 22,000 μmol m^{-2} day^{-1} (see compilation by Upstill-Goddard et al. 2017). However, considering the broad interval of values, it is evident that our mean estimation is near the low end, being also smaller than CH_4 emissions reported in European estuaries and in temperate and boreal rivers where methanogenesis inhibition by sulfate is negligible (Stanley et al. 2016). CH_4 studies conducted in Indian estuaries (Shalini et al. 2006), African rivers and streams (Borges et al. 2015b; Koné et al. 2010; Upstill-Goddard et al. 2017) and in the Amazon River and tributaries (Bartlett et al. 1990; Sawakuchi et al. 2014) also provided higher methane emissions than those in the Guadalquivir estuary. Nevertheless,

these fluvial catchments are inherently different than ours whose suspended particulate matter is mainly of inorganic nature (de la Paz et al. 2007) (~ 80% PIM vs. 20% POM during our sampling period, not shown) and where the oxygen levels would favor aerobic organic matter degradation and CH_4 losses via oxidation, at least during the study time course. Similar values of methane emissions have been found in the brackish section of a Danish estuary (Abril and Iversen 2002) and in a tidal creek of the Bay of Cádiz that receives large anthropogenic nitrogen loads (Ferrón et al. 2007). Moreover, it is important to acknowledge that methane fluxes were computed here using the approach given by Jiang et al. (2008) and our study did not quantify CH_4 ebullition fluxes whose contribution to total CH_4 emissions cannot be precluded during low water periods and transition from high tide to low tide (Baulch et al. 2011).

The mean N_2O air–water exchange during our sampling period was 8.5 (± 8) µmol m^{-2} day^{-1}, which is almost twofold lower than the global median of N_2O fluxes for open water estuaries and equivalent to 18.2 µmol m^{-2} day^{-1} (Murray et al. 2015). Barnes and Upstill-Goddard (2011) provided N_2O fluxes in seven British estuaries on the order of 43.2 µmol m^{-2} day^{-1} and gave an average estimate of 45.7 µmol m^{-2} day^{-1} for European estuaries. Higher N_2O emissions have been also reported in the Schelde estuary (33.6 µmol m^{-2} day^{-1}, de Bie et al. 2002) and in the Seine river (96.5 µmol m^{-2} day^{-1}) (Garnier et al. 2006). In contrast, N_2O fluxes in the Guadalquivir estuary are more comparable to those computed in the Tagus (5.8 µmol m^{-2} day^{-1}), (Gonçalves et al. 2010) and Tamar estuaries (8.03 µmol m^{-2} day^{-1}), (Barnes and Upstill-Goddard 2011), in some tidal Australian estuaries (between 2.3 and 15.9 µmol m^{-2} day^{-1}), (Musenze et al. 2014; Sturm et al. 2016), in African rivers (from 2 to 28 µmol m^{-2} d^{-1}) (Borges et al. 2015b; Koné et al. 2010) and in the Amazon River and floodplain (from 0.25 to 6.0 µmol m^{-2} day^{-1}), (Guérin et al. 2008).

Hence, the estuary behaved as a small CH_4 source and as a moderate N_2O source under the environmental conditions present during the monitoring period. Our results also show that the estuary acts as a net exporter of both gases to the continental shelf of the gulf of Cádiz, as previous studies conducted in the basin had suggested (Ferrón et al. 2010a, b; de la Paz et al. 2015). Further research is still needed to fully characterize CH_4 and N_2O dynamics in this ecosystem, particularly during events of large flooding, which according to our findings, will likely influence the patterns of gas emissions along the estuary and affect the methane and nitrous oxide budgets in the adjacent coastal region.

Acknowledgements This research was funded by the project 1539/2015 from the Spanish Ministry for Agriculture, Food and Environment. The authors are indebted to María Ferrer-Marco, Marta Riera and Antonio Moreno for support in the field work and samples analysis and Manuel Arjonilla for nutrients analysis.

Author contributions IEH conceived the study, contributed to data analysis and interpretation and draft the manuscript. GN and FFP contributed to data analysis interpretation and critical discussion. SF and MdP contributed to analytical design, data calculation and discussion.

References

Abril G, Iversen N (2002) Methane dynamics in a shallow non-tidal estuary (Randers Fjord, Denmark). Mar Ecol Prog Ser 230:171–181

Abril G, Commarieu M-V, Guerin F (2007) Enhanced methane oxidation in an estuarine turbidity maximum. Limnology oceanography 52(1):470–475

Álvarez-Salgado XA, Miller AEJ (1998) Simultaneous determination of dissolved organic carbon and total dissolved nitrogen in seawater by high temperature catalytic oxidation: conditions for precise shipboard measurements. Mar Chem 62(3–4):325–333

Bakker DC, Bange HW, Gruber N, Johannessen T, Upstill-Goddard RC, Borges AV, Delille B, Löscher CR, Naqvi SWA, Omar AM (2014) Air-sea interactions of natural long-lived greenhouse gases (CO_2, N_2O, CH_4) in a changing climate, ocean–atmosphere Interactions of gases and particles, edited, pp 113–169, Springer

Bange HW (2006) Nitrous oxide and methane in European coastal waters. Estuar Coast Shelf Sci 70(3):361–374

Barnes J, Upstill-Goddard RC (2011) N2O seasonal distributions and air-sea exchange in UK estuaries: Implications for the tropospheric N_2O source from European coastal waters. J Geophys Res Biogeosci 116(G1):G01006

Bartlett KB, Bartlett DS, Harriss RC, Sebacher DI (1987) Methane emissions along a salt-marsh salinity gradient. Biogeochemistry 4:183–202

Bartlett KB, Crill PM, Bonassi JA, Richey JE, Harriss RC (1990) Methane flux from the Amazon River floodplain: emissions during rising water. J Geophys Res Atmos 95(D10):16773–16788

Baulch HM, Schiff SL, Maranger R, Dillon PJ (2011) Diffusive and ebullitive transport of methane and n itrous oxidefrom streams: Are bubble-mediated fluxes important? J Geophys Res 116:G04028. https://doi.org/10.1029/2011JG001656

Beaulieu J, Shuster W, Rebholz J (2010) Nitrous oxide emissions from a large, impounded river: the Ohio river. Environ Sci Technol 44(19):7527–7533

Benson BB, Krause D (1984) The concentration and isotopic fractionation of oxygen dissolved in freshwater and seawater in equilibrium with the atmosphere1. Limnol Oceanogr 29(3):620–632

Borges AV, Abril G (2011) Carbon Dioxide and Methane Dynamics in Estuaries. In: Wolanski E, McLusky DS (eds) Treatise on Estuarine and Coastal Science, vol 5. Academic Press, Waltham, pp 119–161

Borges A, Abril G, Darchambeau F, Teodoru CR, Deborde J, Vidal LO, Lambert T, Bouillon S (2015a) Divergent biophysical controls of aquatic CO_2 and CH_4 in the World's two largest rivers. Sci Rep 5:15614

Borges A, Darchambeau F, Teodoru CR, Marwick TR, Tamooh F, Geeraert N, Omengo FO, Guérin F, Lambert T, Morana C (2015b) Globally significant greenhouse-gas emissions from African inland waters. Nat Geosci 8(8):637–642

Borges A, Champenois W, Gypens N, Delille B, Harlay J (2016) Massive marine methane emissions from near-shore shallow coastal areas. Sci Rep 6:27908

Borges AV, Darchambeau F, Lambert T, Bouillon S, Morana C, Brouyère S, Hakoun V, Jurado A, Tseng H-C, Descy J-P, Roland FAE (2018) Effects of agricultural land use on fluvial carbon dioxide,

methane and nitrous oxide concentrations in a large European river, the Meuse (Belgium). Sci Total Environ 610–611:342–355
Borges AV, G Speeckaert, W Champenois, M.I. Scranton & N Gypens (2017) Productivity and temperature as drivers of seasonal and spatial variations of dissolved methane in the Southern Bight of the North Sea, Ecosystems. https://doi.org/10.1007/s10021-017-0171-7
Bouillon S, Yambélé A, Spencer R, Gillikin D, Hernes P, Six J, Merckx R, Borges A (2012) Organic matter sources, fluxes and greenhouse gas exchange in the Oubangui River (Congo River basin). Biogeosciences 9:2045–2062
Brase L, Bange HW, Lendt R, Sanders T, Dähnke K (2017) High resolution measurements of nitrous oxide (N_2O) in the Elbe Estuary. Front Mar Sci 4:162
Bridgham SD, Cadillo-Quiroz H, Keller JK, Zhuang Q (2013) Methane emissions from wetlands: biogeochemical, microbial, and modeling perspectives from local to global scales. Glob Change Biol 19(5):1325–1346
Caballero I, Ruiz J, Navarro G (2018) Multi-platform assessment of turbidity plumes during dredging operations in a major estuarine system. Int J Appl Earth Obs Geoinf 68:31–41
Cai W-J, Wang Y (1998) The chemistry, fluxes, and sources of carbon dioxide in the Estuarine waters of the Satilla and Altamaha rivers, Georgia. Limnol Oceanogr 43(4):657–668
Ciais P et al (2013) Carbon and other biogeochemical cycles. In: Stocker TF (ed) et al Climate Change 2013: the physical science basis. Contribution of WorkingGroup I to the Fifth Assessment Report of the Intergovernmental Panel on Climate Change. Cambridge Univ. Press, Cambridge, pp 465–570
Codispoti LA (2010) Interesting times for marine N_2O. Science 327(5971):1339–1340
Cotovicz LC, Knoppers BA, Brandini N, Poirier D, Costa Santos SJ, Abril G (2016) Spatio-temporal variability of methane (CH_4) concentrations and diffusive fluxes from a tropical coastal embayment surrounded by a large urban area (Guanabara Bay, Rio de Janeiro, Brazil). Limnol Oceanogr 61:S238–S252. https://doi.org/10.1002/lno.10298
de Bie MJ, Middelburg JJ, Starink M, Laanbroek HJ (2002) Factors controlling nitrous oxide at the microbial community and estuarine scale. Mar Ecol Prog Ser 240:1–9
de la Paz M, Gomez-Parra A, Forja J (2007) Inorganic carbon dynamic and air–water CO_2 exchange in the Guadalquivir Estuary (SW Iberian Peninsula). J Mar Syst 68:265–277
de la Paz M, Huertas IE, Flecha S, Ríos AF, Pérez FF (2015) Nitrous oxide and methane in Atlantic and Mediterranean waters in the Strait of Gibraltar: air–sea fluxes and inter-basin exchange. Prog Oceanogr 138(Part A):18–31
Dickson AG (1990) Standard potential of the reaction: $AgCl(s) + 12H_2(g) = Ag(s) + HCl(aq)$, and and the standard acidity constant of the ion HSO_4—in synthetic sea water from 273.15 to 318.15 K. J Chem Thermodyn 22(2):113–127
Díez-Minguito M, Baquerizo A, Ortega-Sánchez M, Navarro G, Losada MA (2012) Tide transformation in the Guadalquivir estuary (SW Spain) and process-based zonation. J Geophys Res Oceans 117(C3):C03019
Díez-Minguito M, Contreras E, Polo MJ, Losada MA (2013) Spatio-temporal distribution, along-channel transport, and post-riverflood recovery of salinity in the Guadalquivir estuary (SW Spain). J Geophys Res Oceans 118(5):2267–2278
Ferrón S, Ortega T, Gómez-Parra A, Forja JM (2007) Seasonal study of dissolved CH_4, CO_2 and N_2O in a shallow tidal system of the bay of Cádiz (SW Spain). J Mar Syst 66(1–4):244–257
Ferrón S, Ortega T, Forja JM (2010a) Nitrous oxide distribution in the north-eastern shelf of the Gulf of Cádiz (SW Iberian Peninsula). Mar Chem 119(1–4):22–32
Ferrón S, Ortega T, Forja JM (2010b) Temporal and spatial variability of methane in the north-eastern shelf of the Gulf of Cádiz (SW Iberian Peninsula). J Sea Res 64(3):213–223
Flecha S, Huertas IE, Navarro G, Morris E, Ruiz J (2015) Air–water CO_2 fluxes in a highly heterotrophic Estuary. Estuaries Coasts 38(6):2295–2309
Garnier J, Cébron A, Tallec G, Billen G, Sebilo M, Martinez A (2006) Nitrogen behaviour and nitrous oxide emission in the tidal Seine River estuary (France) as influenced by human activities in the upstream watershed. Biogeochemistry 77(3):305–326
Gelesh L, Marshall K, Boicourt W, Lapham L (2016) Methane concentrations increase in bottom waters during summertime anoxia in the highly eutrophic estuary, Chesapeake Bay. Limnol Oceanogr 61:S253–S266. https://doi.org/10.1002/lno.10272
Gonçalves C, Brogueira MJ, Camões MF (2010) Seasonal and tidal influence on the variability of nitrous oxide in the Tagus estuary, Portugal. Sci Marina 74(S1):57–66
Grossart H-P, Frindte K, Dziallas C, Eckert W, Tang KW (2011) Microbial methane production in oxygenated water column of an oligotrophic lake. Proc Natl Acad Sci 108(49):19657–19661
Guérin F, Abril G, Tremblay A, Delmas R (2008) Nitrous oxide emissions from tropical hydroelectric reservoirs. Geophys Res Lett 35(6):L06404. https://doi.org/10.1029/2007GL03305
Hamdan LJ, Wickland KP (2016) Methane emissions from oceans, coasts, and freshwater habitats: new perspectives and feedbacks on climate. Limnol Oceanogr 61:S3–S12. https://doi.org/10.1002/lno.10449
Hansen HP, Koroleff F (1999) Determination of nutrients. In: Grasshof K, Kremling K, Ehrhardt M (eds) Methods of seawater analysis. WILEY-VCH, Weilheim, pp 159–228
Havlicek LL, Peterson NL (1977) Effect of the violation of assumptions upon significance levels of the pearson r. Psychol Bull 84(2):373–377
Howarth R, Chan F, Conley DJ, Garnier J, Doney SC, Marino R, Billen G (2011) Coupled biogeochemical cycles: eutrophication and hypoxia in temperate estuaries and coastal marine ecosystems. Front Ecol Environ 9(1):18–26
Huertas IE, Flecha S, Figuerola J, Costas E, Morris EP (2017a) Effect of hydroperiod on CO_2 fluxes at the air-water interface in the Mediterranean coastal wetlands of Doñana. J Geophys Res Biogeosci. https://doi.org/10.1002/2017JG003793
Huertas IE, de la Paz M, Flecha S, Perez FF (2017b) Methane and nitrous oxide air-water fluxes from Doñana wetlands: spatial and temporal variability of emissions. In: Annual meeting of Society of Wetlands Scientists, San Juan, Puerto Rico
Hurkuck M, Althoff F, Jungkunst HF, Jugold A, Keppler F (2012) Release of methane from aerobic soil: an indication of a novel chemical natural process? Chemosphere 86(6):684–689
Jiang LQ, Cai WJ, Wang YC (2018) A comparative study of carbon dioxide degassing in river- and marine-dominated estuaries. Limnol Oceanogr 53:2603–2615. https://doi.org/10.4319/lo.2008.53.6.2603
Keppler F, Hamilton JT, Braß M, Röckmann T (2006) Methane emissions from terrestrial plants under aerobic conditions. Nature 439(7073):187
Keppler F, Boros M, Frankenberg C, Lelieveld J, McLeod A, Pirttilä AM, Röckmann T, Schnitzler J-P (2009) Methane formation in aerobic environments. Environ Chem 6(6):459–465
Kirschke S, Bousquet P, Ciais P, Saunois M, Canadell JG, Dlugokencky EJ, Bergamaschi P, Bergmann D, Blake DR, Bruhwiler L (2013) Three decades of global methane sources and sinks. Nat Geosci 6(10):813
Klüber HD, Conrad R (1998) Inhibitory effects of nitrate, nitrite, NO and N_2O on methanogenesis by Methanosarcina barkeri and Methanobacterium bryantii. FEMS Microbiol Ecol 25(4):331–339

Koné YJM, Abril G, Delille B, Borges AV (2010) Seasonal variability of methane in the rivers and lagoons of Ivory Coast (West Africa). Biogeochemistry 100(1):21–37

Lapierre J-F, del Giorgio PA (2012) Geographical and environmental drivers of regional differences in the lake pCO_2 versus DOC relationship across northern landscapes. J Geophys Res Biogeosci 117:G03015. https://doi.org/10.1029/2012JG001945

Lewis E, Wallace D, Allison LJ (1998), Program developed for CO_2 system calculations, Carbon Dioxide Information Analysis Center, managed by Lockheed Martin Energy Research Corporation for the US Department of Energy

Losada MA, Díez-Minguito M, Reyes-Merlo M (2017) Tidal-fluvial interaction in the Guadalquivir River Estuary: spatial and frequency-dependent response of currents and water levels. J Geophys Res Oceans 122(2):847–865

Maher DT, Cowley K, Santos IR, Macklin P, Eyre BD (2015) Methane and carbon dioxide dynamics in a subtropical estuary over a diel cycle: insights from automated in situ radioactive and stable isotope measurements. Mar Chem 168:69–79

Middelburg JJ, Nieuwenhuize J, Iversen N, Høgh N, De Wilde H, Helder W, Seifert R, Christof O (2002) Methane distribution in European tidal estuaries. Biogeochemistry 59(1–2):95–119

Mintrop L, Pérez FF, González-Dávila M, Santana-Casiano JM, Körtzinger A (2000) Alkalinity determination by potentiometry: Intercalibration using three different methods. Cienc Mar 26(1):23–27

Murray RH, Erler DV, Eyre BD (2015) Nitrous oxide fluxes in estuarine environments: response to global change. Glob Change Biol 21(9):3219–3245

Musenze RS, Werner U, Grinham A, Udy J, Yuan Z (2014) Methane and nitrous oxide emissions from a subtropical estuary (the Brisbane River estuary, Australia). Sci Total Environ 472:719–729

Myhre G et al (2013) Anthropogenic and Natural Radiative Forcing. In: Stocker TF, Qin D, Plattner G-K, Tignor M, Allen SK, Boschung J, Nauels A, Xia Y, Bex V, Midgley PM (eds) Climate Change 2013: The Physical Science Basis. Contribution of Working Group I to the Fifth Assessment Report of the Intergovernmental Panel on Climate Change. Cambridge University Press, Cambridge, pp 659–740

Naqvi S, Bange H, Farías L, Monteiro P, Scranton M, Zhang J (2010) Marine hypoxia/anoxia as a source of CH_4 and N_2O. Biogeosciences 7(7):2159–2190

Nisbet E, Dlugokencky E, Manning M, Lowry D, Fisher R, France J, Michel S, Miller J, White J, Vaughn B (2016) Rising atmospheric methane: 2007–2014 growth and isotopic shift. Glob Biogeochem Cycle 30(9):1356–1370

Poffenbarger HJ, Needelman BA, Megonigal JP (2011) Salinity influence on methane emissions from tidal marshes. Wetlands 31:831–842. https://doi.org/10.1007/s13157-011-0197-0

Ravishankara A, Daniel JS, Portmann RW (2009) Nitrous oxide (N_2O): the dominant ozone-depleting substance emitted in the 21st century. science 326(5949):123–125

Raymond P, Cole JJ (2001) Gas exchange in rivers and estuaries: choosing a gas transfer velocity. Estuaries 24:312–317

Richey JE, Devol AH, Wofsy SC, Victoria R, Riberio MN (1988) Biogenic gases and the oxidation and reduction of carbon in Amazon River and floodplain waters. Limnol Oceanogr 33(4):551–561

Ruiz J, Polo MJ, Díez-Minguito M, Navarro G, Morris EP, Huertas IE, Caballero E, Contreras, Losada MA (2015) The Guadalquivir estuary: a hot spot for environmental and human conflicts. In: Environmental management and governance. Springer, edited, pp 199–232

Ruiz J, Macias D, andG. Navarro(2017) Natural forcings on a transformed territory overshoot thresholds of primary productivity in the Guadalquivir Estuary. Cont Shelf Res. https://doi.org/10.1016/j.csr.2017.09.002

Sansone FJ, Holmes ME, Popp BN (1999) Methane stable isotopic ratios and concentrations as indicators of methane dynamics in estuaries. Global Biogeochem Cycles 13(2):463–474

Saunois M et al (2016) The global methane budget 2000–2012. Earth Syst Sci Data 8:697–751

Sawakuchi HO, Bastviken D, Sawakuchi AO, Krusche AV, Ballester MV, Richey JE (2014) Methane emissions from Amazonian Rivers and their contribution to the global methane budget. Glob Change Biol 20(9):2829–2840

Schade JD, Bailio J, McDowell WH (2016) Greenhouse gas flux from headwater streams in New Hampshire, USA: patterns and drivers. Limnol Oceanogr 61:S1

Schaefer H, Fletcher SEM, Veidt C, Lassey KR, Brailsford GW, Bromley TM, Dlugokencky EJ, Michel SE, Miller JB, Levin I (2016) A 21st-century shift from fossil-fuel to biogenic methane emissions indicated by $^{13}CH_4$. Science 352(6281):80–84

Shalini A, Ramesh R, Purvaja R, Barnes J (2006) Spatial and temporal distribution of methane in an extensive shallow estuary, south India. J Earth Syst Sci 115(4):451–460

Silvennoinen H, Liikanen A, Rintala J, Martikainen PJ (2008) Greenhouse gas fluxes from the eutrophic Temmesjoki River and its Estuary in the Liminganlahti Bay (the Baltic Sea). Biogeochemistry 90(2):193–208

Smith SD (1988) Coefficients for sea surface wind stress, heat flux, and wind profiles as a function of wind speed and temperature. J Geophys Res Oceans 93(C12):15467–15472

Smith LK, Lewis WM, Chanton JP, Cronin G, Hamilton SK (2000) Methane emissions from the Orinoco River floodplain, Venezuela. Biogeochemistry 51(2):113–140

Stanley EH, Casson NJ, Christel ST, Crawford JT, Loken LC, Oliver SK (2016) The ecology of methane in streams and rivers: patterns, controls, and global significance. Ecol Monogr 86(2):146–171

Stocker TF et al (2013) Technical Summary. In: Assessment Report of the Intergovernmental Panel on Climate Change, edited by Stocker TF, Qin D, Plattner G-K, Tignor M, Allen SK, Boschung J, Nauels A, Xia Y, Bex V, Midgley PM Climate Change 2013: The physical science basis. Contribution of Working Group I to the Fifth. Cambridge University Press, Cambridge, pp 33–115

Sturm K, Grinham A, Werner U, Yuan Z (2016) Sources and sinks of methane and nitrous oxide in the subtropical Brisbane River estuary, South East Queensland, Australia, Estuarine. Coastal Shelf Sci 168:10–21

Thompson RL, Sasakawa M, Machida T, Aalto T, Worthy D, Lavric JV, Myhre CL, Stohl A (2017) Methane fluxes in the high northern latitudes for 2005–2013 estimated using a Bayesian atmospheric inversion. Atmos Chem Phys 17:3553–3572

Upstill-Goddard RC, Barnes J (2016) Methane emissions from UK estuaries: re-evaluating the estuarine source of tropospheric methane from Europe. Mar Chem 180:14–23

Upstill-Goddard RC, Barnes J, Frost T, Punshon S, Owens NJ (2000) Methane in the southern North Sea: low-salinity inputs, estuarine removal, and atmospheric flux. Glob Biogeochem Cycle 14(4):1205–1217

Upstill-Goddard RC, Salter ME, Mann PJ, Barnes J, Poulsen J, Dinga B, Fiske GJ, Holmes RM (2017) The riverine source of CH_4 and N_2O from the Republic of Congo, western Congo Basin. Biogeosciences 14(9):2267

Von Fischer JC, Hedin LO (2007) Controls on soil methane fluxes: tests of biophysical mechanisms using stable isotope tracers, Glob Biogeochem Cycle 21(2)

Wanninkhof R (1992) Relationship between wind speed and gas exchange. J geophys Res 97(25):7373–7382
Wilde HPJ, de Bie MJM (2000) Nitrous oxide in the Schelde estuary: production by nitrification and emission to the atmosphere. Mar Chem 69:203–216
Zhang G, Zhang J, Ren J, Li J, Liu S (2008) Distributions and sea-to-air fluxes of methane and nitrous oxide in the North East China Sea in summer. Mar Chem 110(1):42–55